Resolution of complex motion detectors in the central and peripheral visual field

Peter J. Bex and Helle K. Falkenberg

Institute of Ophthalmology, University College London, 11-43 Bath Street, London EC1V 9EL, UK

Received October 7, 2005; accepted December 27, 2005; posted February 10, 2006 (Doc. ID 65182)

We examine how local direction signals are combined to compute the focus of radial motion (FRM) in random dot patterns and examine how this process changes across the visual field. Equivalent noise analysis showed that a loss in FRM accuracy was largely attributable to an increase in local motion detector noise with little or no change in efficiency across the visual field. The minimum separation for discriminating the foci of two overlapping optic flow patterns increased in the periphery faster than predicted from the resolution for a single FRM. This behavior requires that observers average numerous local velocities to estimate the FRM, which enables resistance to internal and external noise and endows the system with the property of position invariance. However, such pooling limits the precision with which multiple looming objects can be discriminated, especially in the peripheral visual field. © 2006 Optical Society of America

OCIS codes: 330.4150, 330.5510, 330.6130, 330.6790, 330.7310.

1. INTRODUCTION

Physiological[1–3] and behavioral[4] studies have shown that the receptive fields of early visual mechanisms are highly selective for a limited range of stimulus attributes, such as spatial frequency and direction of movement, and that they are relatively small, responding to structure within only a very limited region of the visual field. However, the visual system is required to produce useful information about spatially extensive motion, such as ego motion or object movement, which cannot be derived directly by local mechanisms and must be inferred by combining a number of local inputs across visual space. Such a view is consistent with a variety of recent behavioral,[5–19] electrophysiological,[20–27] and imaging[28,29] studies that propose that local motion signals form the first stage within a hierarchy of motion processors with increasing receptive field size and selectivity for increasingly complex forms of global motion.

Self-motion and the motion of objects in the real world give rise to characteristic patterns of retinal motion, known as optic flow.[30,31] The perception of optic flow is typically studied in the laboratory with sparse random dot stimuli that give rise to a compelling sense of realistic motion[32] (see Ref. 33 for a review). The focus of radial motion (FRM) in such computer-generated random dot stimuli can be estimated with an accuracy of around 0.5°.[34] While in principle the FRM could be calculated from the intersection of the velocity vectors of just two dots,[35–38] there is convincing evidence that observers integrate the local directions across the stimulus. For example, sensitivity to the FRM increases with the number of target dots by a power law ($\sqrt{N}$), reaching an asymptote at around 30 dots.[34] This compares favorably with direction discrimination[39–43] and global motion coherence thresholds in planar dot fields, which also saturate at relatively small dot numbers.[42] Warren *et al.*[44] measured sensitivity to the FRM in random dot stimuli in which noise was added to the local direction of each dot (termed random walk). Sensitivity fell gradually from around 0.5° for noise-free stimuli to around 1.5° when the directional bandwidth was 45° and was still detectable when the bandwidth was as great as 135°, indicating that complex motion detectors can average many directional signals. Sensitivity to the FRM is highest when the center of expansion is present in the stimulus[45] consistent with the precision with which the intersection of element vectors can be computed.[46] There is a smaller advantage when the center of expansion is at or near the fovea,[46] which probably arises from the higher resolution of parafoveal vision. Optic flow contains speed as well as directional information across the field that could also be used to estimate the FRM. Randomizing the element directions while preserving their speed distribution produces chance performance in estimating the FRM, indicating that subjects do not use the speed distribution. Conversely, randomizing the speed information while preserving the directional distribution has negligible effect on FRM estimation.[44] Similarly, eliminating the speed gradient (acceleration) by reducing element lifetime to two frames has little effect on FRM estimation.[44] These results suggest that the FRM is estimated in random dot patterns mostly by integrating the directions of elements, regardless of their speeds.

A number of computational models of complex motion processing have been advanced to estimate the direction of heading of a moving observer in static and dynamic environments. In principle, direction of heading can be inferred at the intersection of image velocity vectors,[35–38] by encoding first- or second-order spatial derivatives from the flow field,[47] or from relative motion information contained in motion parallax[35,48–52] and in the relative motions of objects at varying depths and speeds[53] in the scene (see Ref. 54 for a review). Typically, eye movement and postural effects are compensated by the subtraction of efference copy from the flow field to derive egocentric direction of heading from retinocentric optic flow.[55–57]

Electrophysiological[20–24] studies of neurons in area MST of primates have identified neurons with large receptive fields that are selective for radial, rotational, and spiral patterns of optic flow. These properties suggest that MST plays a key role in estimating the direction of self-motion. Furthermore, microstimulation[58,59] of MST neurons can bias the perceived direction of complex motion, confirming that these neurons can contribute to decisions about the direction of heading. While some MST neurons are selective for a particular form of complex motion, in many cases the responses are relatively invariant to the precise location of the center of complex motion within the receptive field—a phenomenon termed position invariance,[20,21,24] which may serve partially to compensate for fixation change.[60] Analogous evidence for position invariance has been reported in behavioral studies of motion processing. For example, adapting to a field of expanding motion produces a robust contracting motion aftereffect (MAE) (see Mather *et al.*[61] for a review of the long history of MAE research). Assuming stable fixation, during adaptation the region of visual space to the left of the center expansion experiences exclusively leftward motion—so a test pattern presented in this location should appear to drift rightward. However, random noise patterns presented in this location often appear to contract, providing behavioral evidence for position invariance.[15] Position invariance means that accurate FRM estimation can be based not on the activity of a single optic flow detector but on the activity of a population of optic flow detectors with overlapping receptive fields.

While position invariance allows an organism to resist changes in retinotopic flow fields with transient changes in posture and gait, it reduces the precision with which the direction of heading can be calculated. Models of optic flow and FRM estimation depend on integrating the responses of many directionally selective motion detectors with small receptive fields, typically modeled with motion energy sensors[62–64] and associated with neurons in area V1. This approach incorporates competing limitations: Accurate estimation of the direction of heading depends on the stable retinotopic locations of motion detectors selective for different speeds and directions. However, position invariance requires flexible integration of motion detectors selective for different speeds and directions with somewhat less regard for their retinotopic locations. In this study we use one old and two novel approaches to estimate the precision with which observers can estimate the FRM in random dot stimuli in an attempt to understand the processes of direction detection and motion pooling that support the perception of optic flow. We apply these techniques at a number of retinal locations to examine how optic flow processing changes across the visual field. In the first task, we measure the overall precision of motion integration by asking observers simply to position a cursor at the apparent FRM at a number of retinal locations. In a second experiment, we use an equivalent noise (EN) paradigm to examine how intrinsic noise and efficiency limit the estimation of the FRM. This technique allows us to separate the contribution of local element uncertainty and global element integration in the estimation of the FRM. While spatial resolution declines rapidly in the peripheral visual field,[65,66] motion sensitivity is relatively invariant to retinal eccentricity for acuity-corrected targets.[67–69] We perform EN analysis as a function of retinal eccentricity to examine how intrinsic noise and sampling efficiency for optic flow perception vary across the visual field. The property of position invariance requires that the visual system base its estimate of the FRM on the pooled responses of a population of overlapping (position-invariant) receptive fields. In a final experiment, we formulate and test the hypothesis that the ability to discriminate one from two (or more) directions of heading (foci of radial motion) in the same location must be compromised by such pooling.

2. GENERAL METHODS: STIMULI

Stimuli were generated in MATLAB running on a PC microcomputer using software adapted from the PsychToolbox routines[70,71] and were displayed with a GeForce4 MX440 graphics card on a LaCieElectron22 monitor with a mean luminance of 50 cd/m^2 and a frame rate of 75 Hz. The gamma function was measured with a Minolota CS100 photometer and was corrected directly in the graphics card's control panel to produce linear 8 bit resolution per color, without any loss of monochrome resolution that occurs with software lookup tables. The display measured 36° horizontally (1152 pixels) and 27° vertically (864 pixels) and was 57 cm from the observer in a dark room.

Stimuli were 8° square fields (256×256 pixels) of 200 black and white, limited lifetime Gaussian dots of 50% Michelson contrast that formed a global pattern of radial motion (expansion or contraction). We used 200 limited lifetime dots because FRM sensitivity is fully saturated at this dot number.[34] Illustrations of the stimuli are shown in Fig. 1; in these images two successive movie frames (each containing only 100 dots for clarity) have been summed to illustrate radial patterns of global motion. There was an equal number of black and white dots to ensure that the mean luminance of the stimulus was the same as that of the background and to avoid potential masking effects from a DC component at the scale of the pattern. The Michelson contrast of the dots was 50% (a) because, at this contrast, motion sensitivity (determined by motion coherence thresholds) was invariant at the eccentricities tested in the present task[72] and (b) because overlapping elements summed, so the use of elements of nonunit contrast reduced the probability of lookup table overflows. The lifetime of the dots was fixed at three movie frames (80 ms) for three reasons: (a) to prevent observers from tracking single dots over time, (b) to prevent large density changes that occur as dots cluster in the center of the image with contracting motion, and (c) because FRM sensitivity is relatively invariant to element lifetime.[44] To support antialiasing, the dots were spatial Gaussians of the form

$$L(x,y) = \exp\left(-\frac{x^2+y^2}{2\sigma^2}\right), \tag{1}$$

where σ, the standard deviation, was 3.75 arc min. Subpixel antialiasing to 0.1 pixel accuracy was achieved by

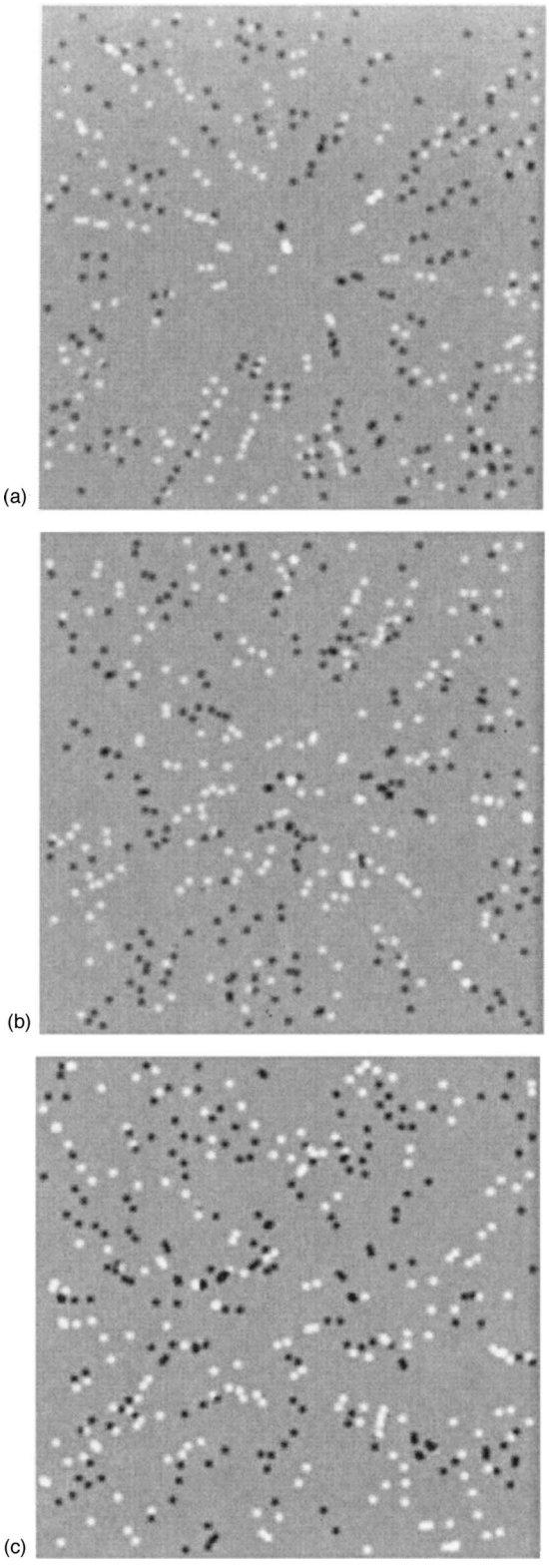

Fig. 1. Illustrations of the stimuli. Each image is the sum of two consecutive frames from illustrative movies from the experiments. Elements in the first frame are randomly positioned; elements in the second frame are positioned relative to those in the first frame to generate an expanding/contracting radial flow field. (a) Noiseless radial motion. In (b) the x location of each element is subject to positional noise (experiment 2). There are two foci of radial motion in (c): half the dots (at random) are displaced relative to a focus 32 pixels to the left of center, and the other half are displaced relative to a focus 32 pixels to the right of center.

generating a 10×10 grid of elements with combinations of 0.0–0.9 pixel offsets in the x and y directions. The direction of radial motion (expansion or contraction) was randomly assigned each trial to minimize the buildup of direction-specific aftereffects. At the start of each trial, the dots were assigned a random starting location, a random black or white contrast polarity (which was fixed for the trial), and a random age between one and three movie frames (to ensure that all dots did not expire simultaneously). On odd video frames of the 75 Hz monitor, the locations of the dots were updated. To generate expanding or contracting motion with a realistic speed gradient, the speed and direction of each dot were calculated by adding ±90° (+90° for expansion, −90° for contraction) to the spatial displacement calculated to produce rigid rotational motion. The dot speed at the half-radius distance was 3.75 deg/s. Dots that fell outside the 8° window and dots whose lifetime exceeded three movie frames were randomly repositioned in the image and assigned a zero age. On even video frames, the stimulus on screen was replaced with the newly calculated movie frame. Movies were presented for 507 ms (19 movie frames; 38 video frames), with abrupt onset and offset. At this duration, direction of heading performance has reached asymptotic levels.[73] A prominent fixation point was provided throughout each run. The fixation point and the location of the stimulus on screen were adjusted so that the center of the stimulus was presented at eccentricities ranging from 0° (foveal) up to 16° in the upper, lower, nasal, or temporal visual field of the observer's dominant eye (the temporal visual field was not tested at 16°, to avoid the blind spot). An eyepatch was worn to occlude the nondominant eye. To ensure compliant fixation, the observer's direction of gaze was monitored with a 50 Hz Cambridge Research System Eye Tracker (www.crsltd.co.uk). If the observer's fixation strayed beyond 1° from the fixation point during the stimulus presentation, auditory feedback was provided and the trial was discarded and repeated at a random point later in the run.

3. EXPERIMENT 1: PERCEIVED DIRECTION OF HEADING AS A FUNCTION OF ECCENTRICITY

Stimuli were the same as those in Section 2 (a 507 ms movie of 200 limited lifetime, black and white, random dots whose velocities formed a global pattern of expanding or contracting motion). The FRM (expansion or contraction) of the radial motion was selected to fall at a random location within the central 4° of the 8° field. The observers' task was to maintain fixation on the fixation mark while the stimulus was present (with compliance enforced by the eye tracker), then, with a mouse, to move the tip of a cursor to the apparent FRM and press the mouse button. The cursor was extinguished during stimulus presentation and reappeared at the fixation point at stimulus offset. This prevented observers from using the cursor as a reference point while the stimulus was present and required similar hand movements on all trial repetitions. Free viewing was permitted during this response section of the task. In pilot runs we found that this relaxation of enforced fixation removed any possibility

that the accuracy of cursor placement would depend on the visibility of the cursor. The 8° diameter stimulus was centered at 4° and 8° in the nasal, temporal, upper, and lower visual field in random order in a single run. Each location was tested a minimum of five times in random order.

Results. Figure 2(a) shows radial plots of the perceived location of the FRM at each eccentricity for three observers as shown in the legend. The data have been corrected for the positional randomization in the experiment to center the data on the test locations (recall that the actual FRM was randomly positioned within the central $4° \times 4°$ of the $8° \times 8°$ stimulus). Figure 2(b) shows precision errors (the distance between the actual and perceived FRM) as a function of eccentricity. Observers were able to identify the direction of heading to within 0.5°–1.2°, in good agreement with previous estimates.[34] There was a modest loss of accuracy with eccentricity, also in line with previous studies.[46] There was no evidence of any overall bias to perceive the FRM from any particular direction, e.g., relative to the fovea, possibly because the FRM was present in the display in all cases. In Section 4 we employ an EN paradigm to examine the underlying changes in visual processing in the peripheral visual field that may account for this reduction in accuracy in the peripheral visual field.

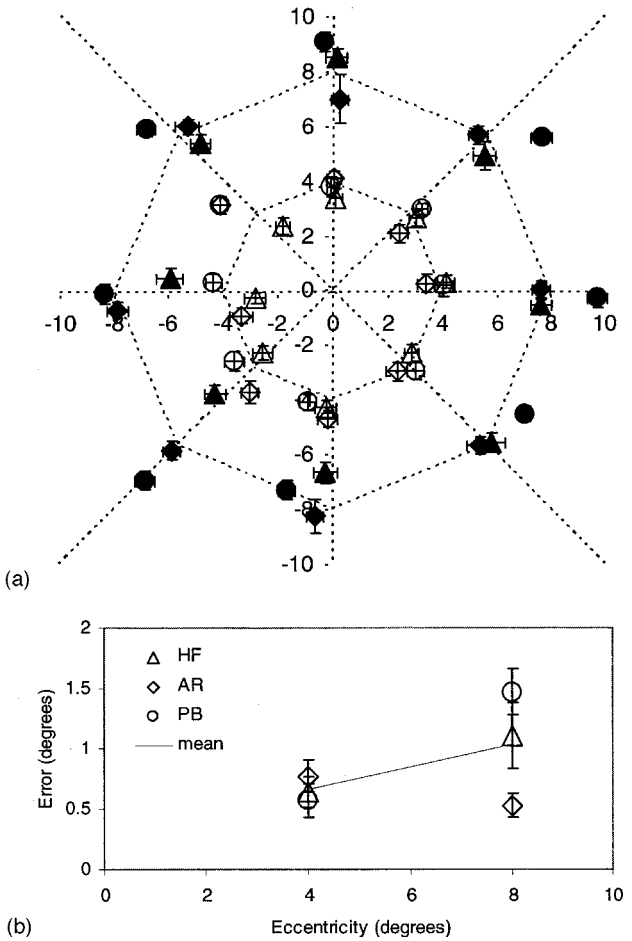

Fig. 2. (a) Radial plot of direction of heading accuracy as a function of retinal locus. Retinal eccentricity from the fovea is plotted in degrees from the center of the figure; the direction is coded compatibly with the visual field. Each data point shows the mean and horizontal and vertical standard deviations of five repetitions of a pointing task, relative to the intersection of the axes. (b) Mean distance between the perceived and the actual focus of radial motion (FRM) averaged across all eight retinal loci at 4° and 8° eccentricity.

4. EXPERIMENT 2: ELEMENT NOISE AND GROUPING EFFICIENCY

At least two factors could limit the precision with which the FRM can be calculated from random dot motion stimuli. In principle, FRM detection requires that observers first detect the velocity vectors of individual dots, then integrate as many of those vectors as possible to maximize efficient integration of the information present in the stimulus. The direction pointing task in experiment 1 is not able to disentangle changes in these factors, which could include improvements in one that fail to compensate for deficits in the other. We adopt an EN paradigm first developed by Barlow[74] and adapted to study the perception of blur,[75] orientation,[76] and motion.[43] On the assumption that visual performance is limited by internal noise in the visual system,[77] the EN paradigm exploits the additivity of variance in the stimulus and variance in the visual system, so that thresholds can be expressed as

$$\sigma_{\mathrm{FRM}} = \sqrt{\frac{\sigma_{\mathrm{int}}^2 + \sigma_{\mathrm{ext}}^2}{N}}, \tag{2}$$

where σ_{FRM} represents FRM discrimination threshold, σ_{int} internal noise in the visual system, σ_{ext} external noise in the stimulus, and N the sampling efficiency, i.e., the number of samples or the proportion of the stimulus that supports the observer's response. We adapted the EN paradigm for FRM estimation by measuring the minimum offset from the center of the stimulus required for observers to indicate the direction of the FRM offset in a two-alternative, forced-choice task. Stimuli were the same as those in Section 2 (a 507 ms movie of 200 limited lifetime, black and white, random dots whose velocities formed a global pattern of expanding or contracting motion), except that the location of the FRM was displaced left or right of center. Once the trajectory of each dot was calculated, a positional offset was added to the horizontal location of each dot. The magnitude of the positional offset for each dot was drawn from a Gaussian distribution with zero mean and a standard deviation that was systematically varied from 0.0625° to 4°. Figure 1(b) illustrates a stimulus with positional standard deviation of 1° (32 pixels). The stimuli appeared at 0°, 8°, or 16° eccentricity in the nasal visual field (to avoid the blind spot), randomly interleaved in a single run. The vertical FRM was fixed at the middle of the 8° stimulus, and the horizontal focus was shifted to the left or right of center (at random across trials) under the control of a 3 down, 1 up staircase[78] that adjusted the offset to a level that produced 75% correct trials. The observer's task was to maintain steady fixation (with compliance enforced by an eye tracker) and to indicate whether the center of expansion was to the left or right of center. Feedback was provided following incorrect responses. Staircases for each noise level were randomly interleaved on a single run. Each

staircase terminated after 50 trials or ten reversals, whichever occurred first. The raw data from a minimum of four repetitions were combined and fitted with a cumulative normal function by least chi squares (in which the data are weighted by the binomial standard deviation, calculated from the observed proportion correct and the number of trials tested at each level). FRM discrimination thresholds were estimated from the 75% correct point of the psychometric function, and 95% confidence intervals on this point were calculated with a bootstrap procedure, based on 1000 data sets simulated from the number of experimental trials at each level tested.[79]

Results. Figure 3 shows FRM discrimination thresholds as a function of the standard deviation of horizontal position noise for five observers and their mean performance at three eccentricities, indicated in the legend in Fig. 3(a). Error bars show ±95% confidence intervals. The data show that observers are still able to identify the FRM to within around 2° or so (depending on eccentricity), even at the highest levels of position noise (4° position noise covers the full radius of the display). In line with random walk studies,[44] this performance requires that observers average many motion cues across the display. The curves show EN fits to the data; the parameters of the fits at each eccentricity are plotted in Figs. 3(g) and 3(h). Open symbols show the parameters for the observers (see the legend). 95% confidence intervals on each parameter were estimated with a bootstrap fit of the EN model to the threshold data. For clarity the mean 95% confidence interval for internal noise and sampling efficiency across observers and conditions is shown as the unconnected error bar on the right of each figure. Solid symbols show the mean parameters across the five observers, and the error bars show 1 standard error. With one exception (observer MT), internal noise (parameter σ_{int}) increased with eccentricity, as is clear from the mean data across observers (solid circles). The results for the sampling efficiency (parameter N) were more variable—three observers (PB, HF, and naive observer AR) showed an increase with eccentricity, and two observers (MT and IM, both naive) showed a decrease with eccentricity. The mean across observers showed little consistent change in sampling efficiency with eccentricity.

We were concerned that when the FRM was moved in this experiment, the mean direction of the dot field also shifted. For example, if the center of an expanding dot field were shifted left, the overall field would contain more rightward dots (on the right of the FRM) than leftward dots. In principle, the observer could use this cue instead of the location of the FRM. The magnitude of this cue is unchanged (on average) as the positional variance increased, and yet the results show a clear loss of sensitivity with positional noise, which suggests that observers were not using this cue. Nevertheless, to remove the cue, one observer (PB) repeated the task with a modified paradigm that made this cue unreliable. The task was identical, except that the observer judged whether the FRM was left or right of a probe instead of the center of the stimulus. The location of the FRM and the probe were randomly offset from the center of the stimulus by up to 3°. The magnitude of the random probe offset was selected because it was larger than the highest threshold across observers and conditions. The probe was presented after stimulus offset. The results are shown in Fig. 3(a) (gray symbols and dashed line fit). The fitted parameters were not significantly different (paired t-test, $p > 0.05$) from those obtained under the nonprobe condition and confirm that observers were not using this cue to perform the FRM task.

5. EXPERIMENT 3: DISCRIMINATING TWO-FOCI RADIAL PATTERNS

Experiments 1 and 2 show that, with noiseless stimuli, the FRM can be determined within approximately 0.5° near the fovea. Accuracy falls modestly with eccentricity, and this is largely attributed to elevated uncertainty on the positional vectors of the local elements rather than to any change in the efficiency with which local elements are integrated. Internal position noise increases from around 1.5° at the fovea to around 3.5° at 16° eccentricity. These data and the phenomenon of position invariance suggest that FRM estimation must be based on the pooled responses of a population of radial motion sensors. We speculate that while such averaging reduces the impact of position noise and position invariance, it causes a loss of resolution for discriminating the FRMs of overlapping radial motion fields, which may occur in natural scenes containing multiple objects moving in different directions relative to a mobile observer. In experiment 3 we test this hypothesis. Stimuli were the same as those in Section 2 (507 ms movies of 200 limited lifetime, black and white, random dots whose velocities formed a global pattern of expanding or contracting motion). A standard and a test movie were presented on each trial at the same retinal location (0°, 8°, or 16° eccentricity in the nasal visual field) in random order, separated by a 507 ms blank interval. The standard movie contained a single FRM that defined the velocities of all 200 dots. The test movie contained two foci of radial motion that were horizontally separated. Each focus determined the velocities of half the dots. Figure 1(c) shows an example image with a separation of 64 pixels (2°) between the foci. The spatial separation between the foci was under the control of a 3 down, 1 up staircase[78] that adjusted the separation to a spacing that produced 75% correct trials. The observer's task was to fixate on a central point (with compliant fixation enforced by an eye tracker) and to indicate which interval contained two foci. Feedback was provided following incorrect responses. Staircases for each eccentricity were randomly interleaved on a single run. Each staircase terminated after 50 trials or ten reversals, whichever occurred first. The data from a minimum of four repetitions were combined and fitted as in experiment 2.

Results. Figure 4 shows the spatial separation thresholds for two foci of radial motion as a function of eccentricity for four subjects (indicated by the legend). As eccentricity increased, the threshold separation between two foci increased. Experiments 1 and 2 show that, for noiseless stimuli, direction of heading accuracy fell from 0.5° to 1.2° on average from fovea to 16° eccentricity. Based on these data, we calculate that observers should be able to discriminate two foci that are separated by $\sqrt{2}$ times these distances (i.e., 0.7°, 1.3°, and 1.7°). This pre-

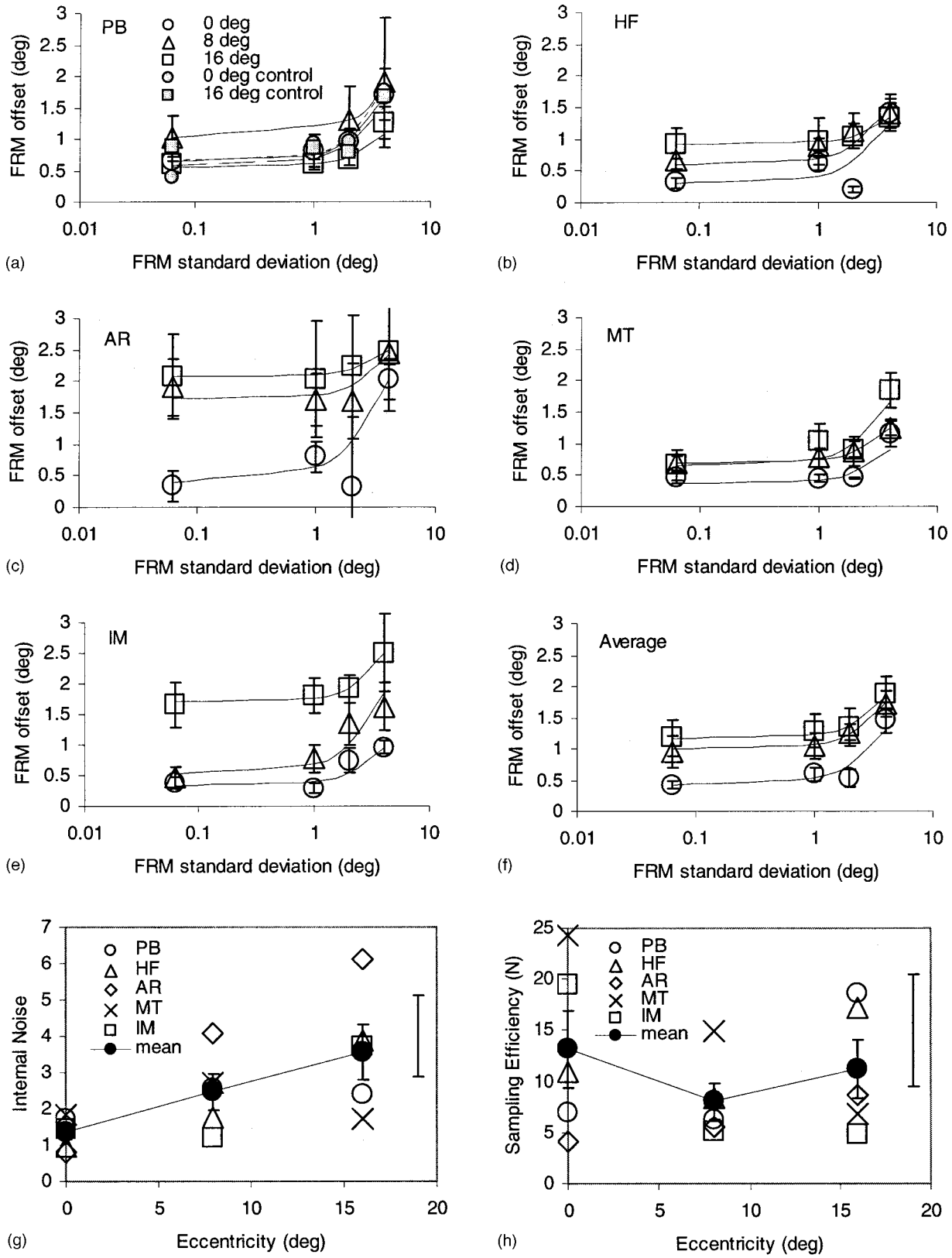

Fig. 3. (a)–(e) FRM discrimination thresholds as a function of horizontal positional noise (applied to each element) at three eccentricities, indicated by the legend. Error bars show 95% confidence intervals. Plots (a)–(e) each shows the data for one observer, and the mean across observers is shown in (f); error bars show 1 standard error. Curves show equivalent noise fits to the data (see the text for details). The internal noise parameter of each fit is plotted as a function of eccentricity for each observer (see the legend) in (g), and the sampling efficiency parameter is plotted in (h). The unconnected error bars on the right of each figure show the mean 95% confidence interval across observers and conditions for each parameter. The solid symbols show the mean value for each parameter across observers, and the error bars show ±1 standard error.

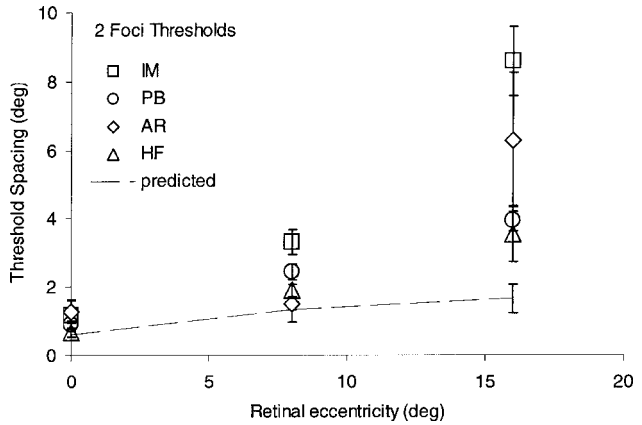

Fig. 4. Two foci of radial motion discrimination thresholds as a function of eccentricity for four observers, indicated by the legend. Error bars show 95% confidence intervals. The dashed line shows the threshold that is predicted from the accuracy with which one focus of radial motion can be discriminated; error bars show ±1 standard error.

dicted performance is plotted in Fig. 4 as the dashed line. Performance was consistently lower than predicted, especially in the peripheral visual field.

6. GENERAL DISCUSSION

Convergent behavioral, electrophysiological, and computational studies agree that visual motion processing proceeds hierarchically, starting with local motion sensors that are selective for image velocity in a small region of visual space. Local motion signals must then be combined at a later stage by global motion integrators with large receptive fields that are selective for more complex forms of pattern motion, such as optic flow. To estimate its direction of heading from the visual flow field, an organism must therefore integrate local velocity vectors across multiple local motion sensors. In this study we examined the precision with which the FRM (expansion/contraction) can be estimated in random dot stimuli. A simple pointing task and a forced choice FRM discrimination task confirmed that observers can identify the direction of heading to within half a degree or so and that accuracy declines modestly in the peripheral visual field. We speculated that the loss of accuracy in the peripheral visual field could arise from a reduction in the accuracy with which the local velocity of each moving element can be determined or by a reduction in the efficiency with which the moving dots can be integrated to represent global radial motion. We used EN analysis to decide between these two factors. EN analysis showed that the decline in direction of heading accuracy in the peripheral visual field was almost exclusively caused by increased uncertainty on element position rather than any consistent change in sampling efficiency. A final task showed that the ability to discriminate single from overlapping pairs of FRMs in radial flow fields declined in the peripheral visual field and that the rate of decline was greater than predicted from the resolution for stimuli containing a single FRM.

A. Position Invariance

Behavioral[15] and electrophysiological[20,21,24] studies show that motion detectors that are selective for optic flow motion are in many cases insensitive to the focus of optic flow—a property termed position invariance. The property of position invariance means that single complex motion detectors cannot identify the FRM with high resolution. The fact that we and others[34] find that the FRM can be determined to within half a degree or so suggests that the responses of a population of complex motion detectors must be compared in order to estimate the overall FRM.

Electrophysiological[80,81] and imaging[29] studies show that cortical receptive field sizes increase in the peripheral visual field. It is tempting to conclude that the increasing receptive field size coupled with position invariance might account for the reduction in FRM sensitivity in the periphery. However, there is no *a priori* reason to assume that an increase in receptive field size should result in a reduction in FRM accuracy: Larger receptive size can integrate more signal velocities, and this might lead to more accurate FRM estimates, especially under noisy conditions. Experiment 2 showed that while there was a steady increase in positional uncertainty in the periphery, there was no consistent change in efficiency (the number of elements used to estimate FRM). This means that although receptive field size increases, the detectors do not appear to integrate a larger number of local motion signals, at least not within the 8° diameter of our stimuli. Experiment 3 showed a rapid falloff in two FRM discrimination thresholds in the peripheral visual field. Both these results suggest that position invariance may increase in the peripheral visual field; it would therefore be interesting to know if this trend were present in primate electrophysiology. The results also suggest that visual processing shifts to larger spatial scales in the peripheral visual field, consistent with our recent finding that global motion processing is low pass tuned for spatial frequency.[19]

B. Foveocentric Bias

Previous studies have shown a bias in the perceived FRM toward the center of the screen.[32,38] We found no evidence in experiment 1 for any bias toward the center of the screen or the fovea, which were coincident in our experiment, nor was there any evident bias toward the center of the stimulus. Figure 2(a) shows that errors were fairly randomly positioned relative to the actual target location and relative to the fovea. It is possible that we failed to show a bias because the center of the FRM was always present in our stimuli and so none of the estimates were based on lamellar flow, which is known to reduce sensitivity.[46] We may not have found biases because it may be harder to detect small observer biases in stimuli with a FRM present than in stimuli in which the FRM is absent. While fixation compliance was enforced during stimulus presentation in our task, observers were allowed to look at the cursor to indicate the FRM during the response section of the task. This avoided confounding any bias in the motion task with biases in the pointing task—the fact that we did not find any bias could therefore mean that biases are greater in the spatial positioning part of the task in paradigms than for fixation compliance in both sections of the task.

C. Direction of Heading, Self-Motion, and Optic Flow

Random dot patterns (especially those composed of limited lifetime elements as in the present study) require that the observer integrate local element velocities in order to identify the FRM. However, at walking speeds[82,83] in real or realistic environments, the path followed by observers wearing optical prisms is consistent with the perceived location of a destination and not with the optic flow generated by self-motion (see Refs. 84–87 for critical reviews of these studies). It is therefore not clear whether observers depend on local velocity integration to guide mobility in everyday experience. Our study was partly motivated by the observation that people with low vision frequently experience mobility difficulties whether they suffer central or peripheral visual field impairment.[88] Our results show that normally sighted observers can detect the FRM with high accuracy in the foveal or peripheral visual field even in conditions of extreme noise and without any visible landmarks present in the scene. This result suggests that if visual guidance for walking were exclusively based on detecting the FRM from local velocities, then visual field loss should produce relatively little effect on mobility and there should be little difference in performance between subjects with central or peripheral scotoma. Clearly, the results do not support this simple prediction, and so factors other than the detection of the direction of heading in optic flow appear to constrain visually guided mobility in observers with low vision.

D. Crowding

Crowding (also known as spatial interference or local contour interaction) refers to the phenomenon that targets that are highly visible in isolation can be rendered indiscriminable in the presence of other nearby targets.[89,90] Several explanations of crowding have argued that crowding is caused by averaging spatial detail within the receptive fields of units selective for complex form.[91–94] According to this view, crowding effects are greater in the peripheral visual field because the spatial extent of averaging (i.e., receptive field size) increases with eccentricity. We were therefore surprised that sampling efficiency (the number of elements divided by the proportion of the stimulus used to perform the direction of heading discrimination) was relatively invariant to eccentricity in experiment 2. This result suggests that as receptive field size increases, the spatial scale of resolution decreases, which is consistent with observed low spatial frequency tuning for crowding in the peripheral visual field[93,95] and for the integration of complex spatial[96] and motion[19] patterns.

Collectively, these data show that the relatively high resolution of FRM detection is achieved by averaging a large number of noisy local velocity estimates within complex motion detectors. The complex motion detectors individually are relatively insensitive to the FRM, and so the estimate of FRM must be based on the distribution of activity across a population of complex motion detectors. Local velocity averaging by global motion detectors enables resistance to internal and external local noise and produces the phenomenon of position invariance; however, it limits the precision with which multiple foci of expansion can be discriminated in overlapping optic flow fields.

ACKNOWLEDGMENTS

This research was supported by The Wellcome Trust and by the Biological and Biotechnical Sciences Research Council.

Correspondence should be addressed to Peter Bex, Institute of Ophthalmology, University College London, 11-43 Bath Street, London EC1V 9EL, UK; phone, +44 207 608 4015; fax, +44 207 608 6983; e-mail, p.bex@ucl.ac.uk.

REFERENCES

1. D. H. Hubel and T. N. Wiesel, "Receptive fields and functional architecture of monkey striate cortex," J. Physiol. (London) **195**, 215–243 (1968).
2. R. H. Wurtz, "Visual receptive fields of striate cortex neurons in awake monkeys," J. Neurophysiol. **32**, 727–742 (1969).
3. P. Schiller, B. L. Finlay, and S. F. Volman, "Quantitative studies of single cell properties in monkey striate cortex. II. Orientation specificity and ocular dominance," J. Neurophysiol. **39**, 1320–1333 (1976).
4. S. J. Anderson and D. C. Burr, "Receptive field size of human motion detection units," Vision Res. **27**, 621–635 (1987).
5. P. Verghese and L. S. Stone, "Combining speed information across space," Vision Res. **35**, 2811–2823 (1995).
6. P. Verghese and L. S. Stone, "Perceived visual speed constrained by image segmentation," Nature (London) **381**, 161–163 (1996).
7. D. Regan and K. I. Beverly, "Looming detectors in the human visual pathway," Vision Res. **18**, 415–421 (1978).
8. T. C. A. Freeman and M. G. Harris, "Human sensitivity to expanding and rotating motion: effects of complementary masking and directional structure," Vision Res. **32**, 81–87 (1992).
9. M. C. Morrone, D. C. Burr, and L. M. Vaina, "2 stages of visual processing for radial and circular motion," Nature (London) **376**, 507–509 (1995).
10. M. C. Morrone, D. C. Burr, and S. Di Pietro, "Cardinal directions for visual optic flow," Curr. Biol. **9**, 763–766 (1999).
11. D. C. Burr, M. C. Morrone, and L. M. Vaina, "Large receptive fields for optic flow detection in humans," Vision Res. **38**, 1731–1743 (1998).
12. K. Gurney and M. J. Wright, "Rotation and radial motion thresholds support a two-stage model of differential-motion analysis," Perception **25**, 5–26 (1996).
13. M. Lappe and J. P. Rauschecker, "An illusory transformation in a model of optic flow processing," Vision Res. **35**, 1619–1631 (1995).
14. R. J. Snowden and A. B. Milne, "Phantom motion aftereffects—evidence of detectors for the analysis of optic flow," Curr. Biol. **7**, 717–722 (1997).
15. R. J. Snowden and A. B. Milne, "The effects of adapting to complex motions: position invariance and tuning to spiral motions," J. Cogn. Neurosci. **8**, 435–452 (1996).
16. P. J. Bex and W. Makous, "Radial motion looks faster," Vision Res. **37**, 3399–3405 (1997).
17. P. J. Bex, A. B. Metha, and W. Makous, "Psychophysical evidence for a functional hierarchy of motion processing mechanisms," J. Opt. Soc. Am. A **15**, 769–776 (1998).
18. P. J. Bex, A. B. Metha, and W. Makous, "Enhanced motion aftereffect for complex motions," Vision Res. **39**, 2229–2238 (1999).
19. P. J. Bex and S. C. Dakin, "Comparison of the spatial-

frequency selectivity of local and global motion detectors," J. Opt. Soc. Am. A **19**, 670–677 (2002).
20. H. A. Saito, M. Yukie, K. Tanaka, K. Hikosaka, Y. Fukada, and E. Iwai, "Integration of direction signals of image motion in the superior temporal sulcus of the macaque monkey," J. Neurosci. **6**, 145–157 (1986).
21. C. J. Duffy and R. H. Wurtz, "Sensitivity of MST neurons to optic flow stimuli. I. A continuum of response selectivity to large-field stimuli," J. Neurophysiol. **65**, 1329–1345 (1991).
22. G. A. Orban, L. Lagae, A. Verri, S. Raiguel, D. Xiao, H. Maes, and V. Torre, "First-order analysis of optical flow in monkey brain," Proc. Natl. Acad. Sci. U.S.A. **89**, 2595–2599 (1992).
23. K. Tanaka and H. Saito, "Analysis of motion of the visual field by direction, expansion/contraction, and rotation cells clustered in the dorsal part of the medial superior temporal area of the macaque monkey," J. Neurophysiol. **62**, 626–641 (1989).
24. M. S. A. Graziano, R. A. Andersen, and R. J. Snowden, "Tuning of MST neurons to spiral motions," J. Neurosci. **14**, 54–67 (1994).
25. J. Kim, K. Mulligan, and H. Sherk, "Simulated optic flow and extrastriate cortex. I: Optic flow versus texture," J. Neurophysiol. **77**, 554–561 (1997).
26. K. Mulligan, J. Kim, and H. Sherk, "Simulated optic flow and extrastriate cortex. II: Responses to bar versus large-field stimuli," J. Neurophysiol. **77**, 562–570 (1997).
27. H. G. Krapp and R. Hengstenberg, "Estimation of self motion by optic flow processing in single visual interneurons," Nature (London) **384**, 463–466 (1996).
28. M. C. Morrone, M. Tosetti, D. Montanaro, A. Fiorentini, G. Cioni, and D. C. Burr, "A cortical area that responds specifically to optic flow, revealed by fMRI," Nat. Neurosci. **3**, 1322–1328 (2000).
29. A. T. Smith, K. D. Singh, A. L. Williams, and M. W. Greenlee, "Estimating receptive field size from fMRI data in human striate and extrastriate visual cortex," Cereb. Cortex **11**, 1182–1190 (2001).
30. J. J. Gibson, *The Perception of the Visual World* (Riverside, 1950).
31. J. J. Koenderink, "Optic flow," Vision Res. **26**, 161–179 (1986).
32. I. R. Johnston, G. R. White, and R. W. Cumming, "The role of optical expansion patterns in locomotor control," Am. J. Psychol. **86**, 311–324 (1973).
33. W. H. Warren, "The state of flow," in *High-Level Motion Processing: Computational, Neurobiological and Psychophysical Perspectives*, K. Watanabe, ed. (MIT, 1998), pp. 315–358.
34. W. H. Warren, Jr., M. W. Morris, and M. Kalish, "Perception of translational heading from optical flow," J. Exp. Psychol. **14**, 646–660 (1988).
35. H. C. Longuet-Higgins and K. Prazdny, "The interpretation of a moving retinal image," Proc. R. Soc. London, Ser. B **208**, 385–397 (1980).
36. N. G. Hatsopoulos and W. H. Warren, "Visual navigation with a neural network," Neural Networks **4**, 303–317 (1991).
37. J. A. Perrone and L. S. Stone, "A model of self-motion estimation within primate extrastriate visual-cortex," Vision Res. **34**, 2917–2938 (1994).
38. W. H. Warren, Jr., and J. A. Saunders, "Perceiving heading in the presence of moving objects," Perception **24**, 315–331 (1995).
39. D. W. Williams and R. Sekuler, "Coherent global motion percepts from stochastic local motions," Vision Res. **24**, 55–62 (1984).
40. S. N. J. Watamaniuk, "Ideal observer for the discrimination of the global direction of dynamic random-dot stimuli," J. Opt. Soc. Am. A **10**, 16–28 (1993).
41. M. O. Scase, O. J. Braddick, and J. E. Raymond, "What is noise for the visual system?" Vision Res. **36**, 2579–2586 (1996).
42. H. Barlow and S. P. Tripathy, "Correspondence noise and signal pooling in the detection of coherent visual motion," J. Neurosci. **17**, 7954–7966 (1997).
43. S. C. Dakin, I. Mareschal, and P. J. Bex, "Local and global limitations on direction integration using equivalent noise analysis," Vision Res. **45**, 3027–3049 (2005).
44. W. H. Warren, Jr., A. W. Blackwell, K. J. Kurtz, N. G. Hatsopoulos, and M. L. Kalish, "On the sufficiency of the velocity field for perception of heading," Biol. Cybern. **65**, 311–320 (1991).
45. R. Warren, "The perception of egomotion," J. Exp. Psychol. **2**, 448–456 (1976).
46. J. A. Crowell and M. S. Banks, "Perceiving heading with different retinal regions and types of optic flow," Percept. Psychophys. **53**, 325–337 (1993).
47. J. J. Koenderink and A. J. van Doorn, "Local structure of movement parallax of the plane," J. Opt. Soc. Am. **66**, 717–723 (1976).
48. M. Lappe, "A model of the combination of optic flow and extraretinal eye movement signals in primate extrastriate visual cortex—neural model of self-motion from optic flow and extraretinal cues," Neural Networks **11**, 397–414 (1998).
49. C. S. Royden, "Computing heading in the presence of moving objects: a model that uses motion-opponent operators," Vision Res. **42**, 3043–3058 (2002).
50. J. H. Rieger and D. T. Lawton, "Processing differential image motion," J. Opt. Soc. Am. A **2**, 354–360 (1985).
51. C. S. Royden, "Mathematical analysis of motion-opponent mechanisms used in the determination of heading and depth," J. Opt. Soc. Am. A **14**, 2128–2143 (1997).
52. E. C. Hildreth, H. B. Barlow, and H. C. Longuet-Higgins, "Recovering heading for visually guided navigation in the presence of self-moving objects," Philos. Trans. R. Soc. London, Ser. B **337**, 305–313 (1992).
53. J. E. Cutting, K. Springer, P. A. Braren, and S. H. Johnson, "Wayfinding on foot from information in retinal, not optical, flow," J. Exp. Psychol. Gen. **121**, 41–72 (1992).
54. E. C. Hildreth and C. S. Royden, "Computing observer motion from optical flow," in *High-Level Motion Processing: Computational, Neurobiological and Psychophysical Perspectives*, K. Watanabe, ed. (MIT, 1998), pp. 269–293.
55. C. S. Royden, M. S. Banks, and J. A. Crowell, "The perception of heading during eye movements," Nature (London) **360**, 583–585 (1992).
56. M. S. Banks, S. M. Ehrlich, B. T. Backus, and J. A. Crowell, "Estimating heading during real and simulated eye movements," Vision Res. **36**, 431–443 (1996).
57. J. A. Crowell, M. S. Banks, K. V. Shenoy, and R. A. Andersen, "Visual self-motion perception during head turns," Nat. Neurosci. **1**, 732–737 (1998).
58. K. H. Britten and R. J. van Wezel, "Electrical microstimulation of cortical area MST biases heading perception in monkeys," Nat. Neurosci. **1**, 59–63 (1998).
59. K. H. Britten and R. J. Van Wezel, "Area MST and heading perception in macaque monkeys," Cereb. Cortex **12**, 692–701 (2002).
60. D. C. Bradley, M. Maxwell, R. A. Andersen, M. S. Banks, and K. V. Shenoy, "Mechanisms of heading perception in primate visual cortex," Science **273**, 1544–1547 (1996).
61. G. Mather, F. A. J. Verstraten, and S. M. Anstis, *The Motion Aftereffect: A Modern Perspective* (MIT, 1998).
62. E. H. Adelson and J. R. Bergen, "Spatiotemporal energy models for the perception of motion," J. Opt. Soc. Am. A **2**, 284–299 (1985).
63. J. P. van Santen and G. Sperling, "Elaborated Reichardt detectors," J. Opt. Soc. Am. A **2**, 300–321 (1985).
64. A. B. Watson and A. J. Ahumada, Jr., "Model of human visual-motion sensing," J. Opt. Soc. Am. A **2**, 322–342 (1985).
65. M. Millidot, "Foveal and extra-foveal acuity with and without stabilized retinal images," Br. J. Physiol. Opt. **23**, 75–106 (1966).
66. J. Rovamo, R. Franssila, and R. Nasanen, "Contrast sensitivity as a function of spatial frequency, viewing distance and eccentricity with and without spatial noise," Vision Res. **32**, 631–637 (1992).

67. S. P. McKee and K. Nakayama, "The detection of motion in the peripheral visual field," Vision Res. **24**, 25–32 (1984).
68. M. J. Wright and A. Johnston, "Spatiotemporal contrast sensitivity and visual field locus," Vision Res. **23**, 983–989 (1983).
69. S. J. Waugh and R. F. Hess, "Suprathreshold temporal-frequency discrimination in the fovea and the periphery," J. Opt. Soc. Am. A **11**, 1199–1212 (1994).
70. D. H. Brainard, "The Psychophysics Toolbox," Spatial Vis. **10**, 433–436 (1997).
71. D. G. Pelli, "The VideoToolbox software for visual psychophysics: transforming numbers into movies," Spatial Vis. **10**, 437–442 (1997).
72. I. Fine, C. M. Anderson, G. M. Boynton, and K. R. Dobkins, "The invariance of directional tuning with contrast and coherence," Vision Res. **44**, 903–913 (2004).
73. J. A. Crowell, C. S. Royden, M. S. Banks, K. H. Swenson, and A. B. Sekuler, "Optic flow and heading judgements," Invest. Ophthalmol. Visual Sci. Suppl. **31**, 522 (1990).
74. H. B. Barlow, "Retinal noise and absolute threshold," J. Opt. Soc. Am. **46**, 634–639 (1956).
75. R. J. Watt and M. J. Morgan, "Spatial filters and the localization of luminance changes in human vision," Vision Res. **24**, 1387–1397 (1984).
76. S. C. Dakin, "Information limit on the spatial integration of local orientation signals," J. Opt. Soc. Am. A **18**, 1016–1026 (2001).
77. D. M. Green and J. A. Swets, *Signal Detection Theory and Psychophysics* (Wiley, 1966).
78. G. B. Wetherill and H. Levitt, "Sequential estimation of points on a psychometric function," Br. J. Math. Stat. Psychol. **18**, 1–10 (1965).
79. D. H. Foster and W. F. Bischof, "Thresholds from psychometric functions: superiority of bootstrap to incremental and probit variance estimators," Psychol. Bull. **109**, 152–159 (1991).
80. D. H. Hubel and T. N. Wiesel, "Uniformity of monkey striate cortex: a parallel relationship between field size, scatter and magnification factor," J. Comp. Neurol. **158**, 295–306 (1974).
81. D. C. Van Essen, W. T. Newsome, and J. H. Maunsell, "The visual field representation in striate cortex of the macaque monkey: asymmetries, anisotropies, and individual variability," Vision Res. **24**, 429–448 (1984).
82. S. K. Rushton, J. M. Harris, M. R. Lloyd, and J. P. Wann, "Guidance of locomotion on foot uses perceived target location rather than optic flow," Curr. Biol. **8**, 1191–1194 (1998).
83. J. M. Harris and W. Bonas, "Optic flow and scene structure do not always contribute to the control of human walking," Vision Res. **42**, 1619–1626 (2002).
84. J. M. Harris, "The future of flow?" Trends Cogn. Sci. **5**, 7–8 (2001).
85. J. M. Harris and B. J. Rogers, "Going against the flow," Trends Cogn. Sci. **3**, 449–450 (1999).
86. M. Lappe, F. Bremmer, and A. V. van ben Berg, "Going against the flow—Reply," Trends Cogn. Sci. **3**, 450 (1999).
87. J. Wann and M. Land, "Heading in the wrong direction. Reply," Trends Cogn. Sci. **5**, 8–9 (2001).
88. J. Lovie-Kitchin, J. Mainstone, J. Robinson, and B. Brown, "What areas of the visual field are important for mobility in low vision patients?" Clin. Vision Sci. **5**, 249–263 (1990).
89. M. C. Flom, F. W. Weymouth, and D. Kahneman, "Visual resolution and spatial interaction," J. Opt. Soc. Am. **53**, 1026–1032 (1963).
90. H. Bouma, "Interaction effects in parafoveal letter recognition," Nature (London) **226**, 177–178 (1970).
91. F. Wilkinson, H. R. Wilson, and D. Ellemberg, "Lateral interactions in peripherally viewed texture arrays," J. Opt. Soc. Am. A **14**, 2057–2068 (1997).
92. L. Parkes, J. Lund, A. Angelucci, J. A. Solomon, and M. Morgan, "Compulsory averaging of crowded orientation signals in human vision," Nat. Neurosci. **4**, 739–744 (2001).
93. S. T. L. Chung, D. M. Levi, and G. E. Legge, "Spatial-frequency and contrast properties of crowding," Vision Res. **41**, 1833–1850 (2001).
94. P. J. Bex and S. C. Dakin, "Spatial interference among moving targets," Vision Res. **45**, 1385–1398 (2005).
95. D. M. Levi, S. Hariharan, and S. A. Klein, "Suppressive and facilitatory spatial interactions in peripheral vision: peripheral crowding is neither size invariant nor simple contrast masking," J. Vision **2**, 167–177 (2002).
96. S. C. Dakin and P. J. Bex, "Local and global visual grouping: tuning for spatial frequency and contrast," J. Vision **1**, 99–111 (2001).